



Contents lists available at ScienceDirect

Journal of King Saud University – Science

journal homepage: [www.sciencedirect.com](http://www.sciencedirect.com)

Original article

# Cytotoxic and molecular assessment against breast (MCF-7) cancer cells with cobalt oxide nanoballs

Rizwan Wahab<sup>a,\*</sup>, Maqsood A. Siddiqui<sup>a</sup>, Javed Ahmad<sup>a</sup>, Quaiser Saquib<sup>a,b</sup>, Abdulaziz A. Al-Khedhairi<sup>a,b</sup><sup>a</sup> Chair for DNA Research, College of Science, Department of Zoology, King Saud University, Riyadh 11451, Saudi Arabia<sup>b</sup> Department of Zoology, King Saud University, Riyadh 11451, Saudi Arabia

## ARTICLE INFO

### Article history:

Received 14 March 2021

Revised 11 April 2021

Accepted 3 May 2021

Available online 8 May 2021

### Keywords:

Cobalt oxide NPs

Cytotoxicity

MCF-7 cells

Reactive oxygen species

RT-PCR

## ABSTRACT

Among various types of cancer, the breast cancer is a very common and widely affected to the human beings especially female candidate. To keep this view the present work was designed to access the cytotoxic and apoptotic responses of breast (MCF-7) cancer cells with cobalt oxide nanoparticles (Co<sub>3</sub>O<sub>4</sub>NPs). The Co<sub>3</sub>O<sub>4</sub>NPs was prepared via solution process and well characterized. The materials crystallinity, size and phase were determined via XRD, whereas the morphology of Co<sub>3</sub>O<sub>4</sub>NPs was analyzed via SEM and TEM respectively. The Co<sub>3</sub>O<sub>4</sub>NPs were spherical in shape with an average diameter of (~33±1). The cytotoxicity rate of breast (MCF-7) cells was much influenced and dose dependent (1, 2, 5, 10, 25, 50 and 100 μL/mL) with Co<sub>3</sub>O<sub>4</sub>NPs confirmed via the MTT and NRU assays. The rate of ROS was increased gradually from 105, 124, 132 and 148 with different concentrations of Co<sub>3</sub>O<sub>4</sub>NPs (10, 25, 50 and 100 μL/mL) with control. The mRNA level of apoptotic markers with Co<sub>3</sub>O<sub>4</sub>NPs was up-regulated and it shows the apoptosis in cells. The study describes the cytotoxicity with Co<sub>3</sub>O<sub>4</sub>NPs in breast (MCF-7) cancer cell were apoptotic gene expression with possible discussion.

© 2021 The Author(s). Published by Elsevier B.V. on behalf of King Saud University. This is an open access article under the CC BY-NC-ND license (<http://creativecommons.org/licenses/by-nc-nd/4.0/>).

## 1. Introduction

Cancer is a divesting disease, which is not only affect the particular organs but disturb to the whole body system (Wahab et al., 2013). It's happens due to uncontrolled progression of normal cells. Several factors influenced such as initiation, promotion and growth etc; are responsible for the transformation of a normal cell to a cancerous one (Bray et al., 2012). Over a number of cancer types, the breast cancer is very common to the entire world and normally diagnosed in female candidates (Nardin et al., 2020). In an estimated value the breast cancer grasp more than one million women's world wide. The periodical statistics data to the incidence of this disease varied widely such as in 2008, about 421,000 cases were recovered for breast cancer, where as in 2009–2010, more than 49,500 women were diagnosed with breast cancer in Europe. From the breast cancer about 11,600 women's and 75 men were

died in 2010. The estimated data caused from this cancer is more than 458,000 women in 2008 worldwide. In 2008, the new cases 184,450 were appeared in persistent stages and this number varies to 230,480 in 2011 in USA. This estimated value is increases day by day and new cases (~268,600) for breast cancer was identified in women, it also detected in men (~2,670) in 2019 (Nardin et al., 2020). An average 42,170 women in the U.S. predictable to die in 2020 (Facts & Figures 2019–2020). A number of therapies have been proposed to cure this devastating disease such as chemotherapy, radiotherapy, proton beam therapy, hormone therapy, targeted drug therapy, clinical trials, cryoablation, immunotherapy etc, that causes so much suffering (Chen et al., 2020, Cammarata et al., 2020, Boing et al., 2020, Li et al., 2020). Including this, surgery is an another option from which the cancer cells were removed from the particular organ of the body such as curative, preventive diagnostic, staging, palliative, supportive, cryosurgery, laser, electro surgery and various others (He et al., 2020, Wahab et al., 2014).

In recent, the nanotechnology, which is a multi-disciplinary area of science, connects with various branches of basic and applied sciences, is a best alternative for to reduce the cancer cells at a very low cost, much effective against cancer cells and not harm to body system. The nanotechnology has privilege to provide a range of fascinating nano and microstructures, which are widely useful to optoelectronic & biological applications (Siddiqui et al., 2015).

\* Corresponding author.

E-mail address: [rwahab@ksu.edu.sa](mailto:rwahab@ksu.edu.sa) (R. Wahab).

Peer review under responsibility of King Saud University.



Production and hosting by Elsevier

Among a large number of metal and metal oxides nanostructures, the cobalt oxide nanostructures ( $\text{Co}_3\text{O}_4\text{NSs}$ ) exhibit a unique properties in electronics, batteries, solar cells, energy storage, imaging, chemical and biological sensing, magnetic, catalysis (Li et al., 2005, Dong et al., 2014, Karuppiyah et al., 2014, Sivachidambaram et al., 2017) etc. Various shapes and sizes endorse and exhibit a surface anisotropy behavior, which influences their magnetic response (Farhadi et al., 2013). The  $\text{Co}_3\text{O}_4\text{NSs}$  also have different properties such as hydrodesulfurization, photo catalyst, oxidation, electrochemical (Askarinejad et al., 2010, Packiaraj et al., 2019) studies. The cobalt oxide nanostructure is a p-type semiconductor, enhance band gap (1.29 to 3.34 eV) energy with enormous photosensitivity including enormous quantum efficiency (Vennela et al., 2019). Over a long range of physicochemical properties and their utilization in various areas, limited studies are available for the biological application of cobalt oxide to diminish the proliferation rate of cancer cells (Jarestan et al., 2020). Towards this direction work related to retardation of cancer cells such as Chattopadhyay et al. describes the role of surface modification of cobalt oxide NPs for the biological activity. For this, different cell lines such as the human lymphocytes, T-cell lymphoma (Jurkat) and oral epithelial cancer (KB) were exposed with surface modified cobalt oxide NPs and achieved their anticancer activity (Chattopadhyay et al., 2012, Mauro et al., 2015, Arsalan et al., 2020, Rauwel et al., 2020). Due to the magnetic and high stability, the cobalt oxide NPs also utilized in hyperthermic treatment. This involves heating of tumor tissues in a temperature below  $50\text{ }^\circ\text{C}$  (Jose et al., 2020). In addition to this, the magnetic NPs can be easily conjugate with DNA, peptides, antibodies, enzymes and other biological molecules to form the nano-bio hybrids (Bossi et al., 2016). The cellular uptake of cobalt oxide NPs was examined via TEM to explore the new insights of mechanisms to entry in cells, distribution and their cellular environment (Papis et al., 2009). The  $\text{Co}_3\text{O}_4\text{NPs}$  were also utilized for the light-induced photodynamic therapy (PDT) and was employed to assess their photo and cytotoxic effects of materials against HepG2 cells (Iqbal et al., 2020).

Over the various applications of  $\text{Co}_3\text{O}_4\text{NPs}$  in different ways, very limited studies are available for to control the cancer cells growth, cellular cytotoxicity, gene expressions are via  $\text{Co}_3\text{O}_4\text{NPs}$ . To keep this view, the core objective of the current work is to elucidate the role of  $\text{Co}_3\text{O}_4\text{NPs}$  against breast cancer cells. The  $\text{Co}_3\text{O}_4\text{NPs}$  were synthesized via solution method with the use of cobalt acetate tetrahydrate ( $\text{Co}(\text{CH}_3\text{COO})_2 \cdot 4\text{H}_2\text{O}$ ) and sodium hydroxide (NaOH) under a very short refluxing temperature. The processed  $\text{Co}_3\text{O}_4\text{NPs}$  crystallinity, particle size and phases were estimated via X-ray diffraction (XRD) pattern, whereas the structural examinations were confirmed via scanning electron (SE) and transmission electron microscopy (TEM) respectively. The chemical functional positions were identified via Fourier transform infra-red (FTIR) spectroscopy. The cytotoxicity study was conducted against breast cancer cells (MCF-7) with using  $\text{Co}_3\text{O}_4\text{NPs}$ . The MCF-7 cells were widely selected because the breast cancer has a major health problem worldwide. The cells viability of cancer cells (MCF-7) were examined with  $\text{Co}_3\text{O}_4\text{NPs}$  with MTT assay. The apoptosis caused with  $\text{Co}_3\text{O}_4\text{NPs}$  was investigated with the accessible real-time polymerase chain reaction (RT-PCR) study also explained why the  $\text{Co}_3\text{O}_4\text{NPs}$  are useful to diminish the growth rate of cancer cells.

## 2. Experimental

### 2.1. Material and methods

#### 2.1.1. Synthesis of cobalt oxide nanoparticles ( $\text{Co}_3\text{O}_4\text{NPs}$ )

The  $\text{Co}_3\text{O}_4\text{NPs}$  were formed through cobalt acetate tetra hydrate ( $\text{CH}_3\text{COO})_2\text{Co} \cdot 4\text{H}_2\text{O}$ ) and sodium hydroxide (NaOH). The chemicals

for the formation of NPs were acquired from Sigma Aldrich chemical Co., USA and used as received. Acetate salt of cobalt and alkali NaOH were assorted in 100 mL of deionized double distilled water (DDDW) with a final concentration of 15 mM (0.18681 g) and 0.2 M (0.2 g), respectively, with the constant stirring conditions for  $\sim 20\text{--}30$  min. The solution pH was measured (corning  $\text{p}^{\text{H}}$  meter 430 red, cole-parmer, U.S.A) and it reaches to 12.79. Once cobalt salt was completely dissolved, the solution was refluxed at  $\sim 90\text{ }^\circ\text{C}$  for 60 min in a refluxing pot. The solution color turns from red to black with increase of temperature of refluxing pot. When the reaction was completed, the formed precipitated product was kept for cooling at room temperature for about  $\sim 24$  h. The obtained product was transferred in a centrifuge tubes ( $\sim 50$  mL capacity) and centrifuge (Eppendorf, 5430R, Centrifuge, Germany). The solution was centrifuged at 3000 rpm for 3 min and dried at room temperature in a glass petri dishes. The powder was analyzed in terms of their morphological and chemical characteristics.

#### 2.1.2. Characterizations of synthesized material

The prepared powder crystallinity, phases, crystallite size were identified via XRD (PAN alytical XPert Pro, U.S.A.) with  $\text{Cu}_{\text{K}\alpha}$  source ( $\lambda = 1.54178\text{ \AA}$ ) from  $20$  to  $70^\circ$  with  $6^\circ$  angle rotation/min speed. The morphology of synthesized product was analyzed via SEM (JSM –6380 LA, Japan). For the analysis of SEM, synthesized product was homogeneously sprinkled on a black colored carbon tape and forms a layer. The cobalt oxide coated sample carbon tape was transferred to the specialized glass chamber for sputtering with thin conducting layer of platinum (pt) for 3 s to enhance the conductance of the material. Further the morphological evaluation was also confirmed via TEM (JEOL, JEM JSM 2010, Japan) and the procured morphological images were collected at 100 kV current. The chemical functional identification of synthesized  $\text{Co}_3\text{O}_4\text{NPs}$  was analyzed via FTIR (Perkin Elmer-FTIR Spectrum-100, U.S.A.) spectroscopy ranges from  $400$  to  $4000\text{ cm}^{-1}$ . For this, very small amount of the powder was used for FTIR analysis, mixed with KBr to form the pellet under high-pressure ( $\sim 4$  tons). The pellet was fixed to the sample holder and analyzed the FTIR at room temperature.

### 2.2. Cell culture (MCF-7 cells) and treatment of cobalt oxide NPs

The breast cancer cells (MCF-7) was grown in a medium (DMEM/MEM) including 12% fetal bovine serum (FBS), 0.2% sodium bicarbonate, and antibiotic-antimycotic solution (100 X, 1 mL/100 mL) with moist environment (5%  $\text{CO}_2$  & 95%  $\text{O}_2$ ) at  $37\text{ }^\circ\text{C}$ . Earlier for the experiments, the cells viability were evaluated by trypan blue dye as per the protocol (Siddiqui et al., 2008) and shows the viability more than 95% were only used in the study. The cells were employed between 10 and 12 passages to treat the cells with nanostructures. The  $\text{Co}_3\text{O}_4\text{NPs}$  were used at high concentration and then subsequently diluted at desired different concentrations for the exposure of cells. The cells were plated in 6-well or 96-well plates as per the experimental requirement.

### 2.3. Reagents and consumables for the biological study

The MTT [3-(4, 5-dimethylthiazol-2-yl)-2, 5 diphenyltetrazolium bromide], was obtained from Sigma Chem.Co.USA and cast-off without any further modification except dilution, besides this the Dulbecco's Modified Eagle Medium (DMEM) and MEM culture medium, antibiotics-antimycotic and FBS were bought from Invitrogen, USA. The plastic wares and other consumables products for cells culture were used from Nunc, Denmark.

## 2.4. MTT assay

Cancer cells viability with (treated) and without  $\text{Co}_3\text{O}_4\text{NPs}$  (control) were accessed via MTT assay as per the previous followed protocol (Siddiqui et al., 2008, Mosmann, 1983). Initially, cells were cultured in a specialized 96 well plates (rate of  $1 \times 10^4/\text{well}$ ) with permissible to follow for 24 h at  $37^\circ\text{C}$  with humidified environment. The cells were intermingled with  $\text{Co}_3\text{O}_4\text{NPs}$  from 1 to  $100 \mu\text{g}/\text{mL}$  for 24 h. When the cells were completely inter mixed in well plates, stock solution of MTT (5 mg/mL in PBS) was amalgamated with rate of  $10 \mu\text{L}/\text{well}$  in  $100 \mu\text{L}$  of cell suspension and further incubated for 4 h. After the completion of incubation period, the well plate's solution was with draw from the pipette and in these wells  $\sim 200 \mu\text{L}$  of DMSO was added for to aspirate the formazan product and mixed gently. The optical characteristic of the solution was measured at 550 nm with micro-plate reader (Multiskan Ex, Thermo Scientific, Finland). The control cells were also employed as a reference and to run with the same conditions. The value of maximum absorbance depends upon the employed solvent in sample solution and the level of viability of cells % was calculated as per the equations mentioned below:

$$\% \text{ viability} = [(\text{total cells} - \text{viable cells}) / \text{total cells}] \times 100$$

## 2.5. NRU assay

The cytotoxic assessment was also confirmed with and without  $\text{Co}_3\text{O}_4\text{NPs}$  via neutral red uptake (NRU) assay as per the previously described procedure (Borenfreund and Puerner, (1985, Siddiqui et al., 2010). The MCF-7 cells ( $1 \times 10^4/\text{well}$ ) cells were sowed in a specified 96 well plates. Once the cells were completely grown (after 24 h) were exposed to desired conc ( $1-100 \mu\text{g}/\text{mL}$ ) of  $\text{Co}_3\text{O}_4\text{NPs}$  and kept for 24 h in an incubator. When the exposure was completed, cells were further incubated in NR medium ( $50 \mu\text{g}/\text{mL}$ ) for 3 h. Thereafter, cells were washed and dye was extracted in 1% acetic acid and 50% ethanol solution. The develop color was read at 540 nm.

## 2.6. Generation of reactive oxygen species (ROS)

The ROS was measured with 2, 7-dichloro dihydrofluoresce in diacetate (DCFH-DA; Sigma Aldrich, USA) dye as a fluorescence agent as per the previously described method (Zhao and Riediker, 2014). Once the cells were exposed with the material for 24 h and then after, cells were rinsed well with PBS and further nurtured for 30 min in DCFH-DA ( $20 \mu\text{M}$ ) in dark place at  $37^\circ\text{C}$ . When the reaction of DCFH-DA with cells control and treated (with  $\text{Co}_3\text{O}_4\text{NPs}$ ) cells completed, cells were examined with using fluorescence microscope.

## 2.7. mRNA expressions with cancer cells (MCF-7)

The RNA isolation was performed with cultured cells of MCF-7 cells in a 6-well plates control and treated sample of  $\text{Co}_3\text{O}_4\text{NPs}$  at concentration of  $50 \mu\text{g}/\text{mL}$  for 24 h. The RNA was mined from RNeasy mini Kit (Qiagen) as according to manufacturer's protocol. The cDNA was synthesized from treated and untreated cells taking  $1 \mu\text{g}$  of RNA by Reverse Transcriptase kit using MLV reverse transcriptase (GE Health Care, UK) as per the manufacturers' protocol. The RT-PCR was performed on Roche® Light Cycler®480 (96-well block) (USA) following the cycling program recommended.  $2 \mu\text{L}$  ( $40 \text{ ng}$ ) of cDNA template included the  $20 \mu\text{L}$  volume to this reaction mixture (Huang et al., 2021, Bejarbaneh et al., 2020).

## 3. Result and discussion

### 3.1. X-ray diffraction pattern (XRD)

Fig. 1 shows the XRD of processed powder via solution process. The XRD pattern defines the crystallinity, crystallite size and phases of the powder material. The well assigned peaks were identified in XRD spectrum and is related to the face centered cubic (FCC) structures and well matched with the JCPDS card No. 76-1802 with  $\text{Co}_3\text{O}_4$ . The peaks and their positions such as  $31.26^\circ$  (220),  $36.84^\circ$ ,  $38.59^\circ$ ,  $44.83^\circ$ ,  $55.68^\circ$ ,  $59.38^\circ$ ,  $65.25^\circ$  illustrates the lattice plane of 220 and 311 for  $\text{Co}_3\text{O}_4$  crystal (Fig. 1) and well justified with the previously published literature of pure  $\text{Co}_3\text{O}_4$  (Divyapriya et al., 2019, El-Dossoki et al., 2020). The intense peak indicates that powder exhibit good crystallinity, small particles size etc (Cullity 1978). The particles size was found to be  $\sim 33 \text{ nm}$ , calculated with using sherrer formula. The obtained X-ray spectrum shows only the  $\text{Co}_3\text{O}_4$  peaks without any other impurities, which indicates the purity of the sample.

### 3.2. Morphological results of $\text{Co}_3\text{O}_4\text{NPs}$

#### 3.2.1. (a) SEM results

The morphology was examined for the processed powder with SEM images and presented as Fig. 2. From the low magnified image (Fig. 2a-b) of  $\text{Co}_3\text{O}_4\text{NPs}$ , it seems that small nanostructures were arranged with the collection of several tiny particles and it seems that these NPs are linked composed and from a spheres shaped structure. Further for more clarification of an individual particle, shape and size of NP was confirmed at high magnified image (Fig. 2c). From recovered image designates that estimated diameter of each individual particle is in range of  $\sim 33 \pm 1 \text{ nm}$  (Fig. 2d). The obtained SEM analysis is well justified and in consistent with the XRD (Fig. 1).

#### 3.2.2. (b) TEM results

For more authentic observation, the grown powder was also analyzed with TEM at an above described procedure in section 2.2 and the obtained data is presented as Fig. 3. TEM image is also in consistent with the SEM images. Number of several nanometer scale particles (NPs) is seen and size of an individual NP ranges to  $\sim 33 \pm 1 \text{ nm}$ . The obtained image confirms the spherical shaped

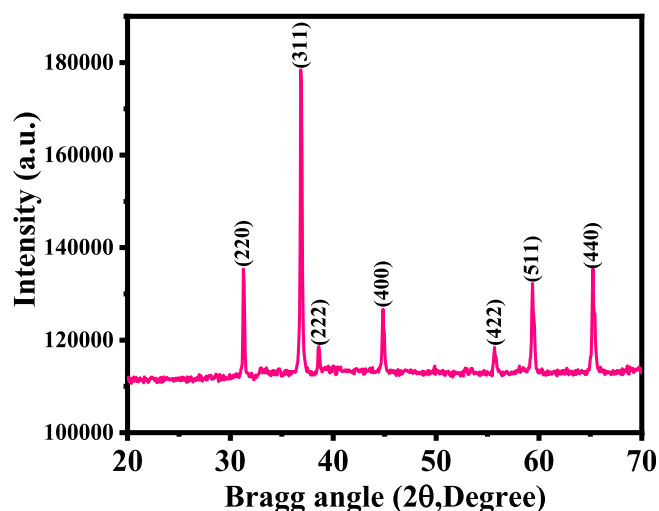
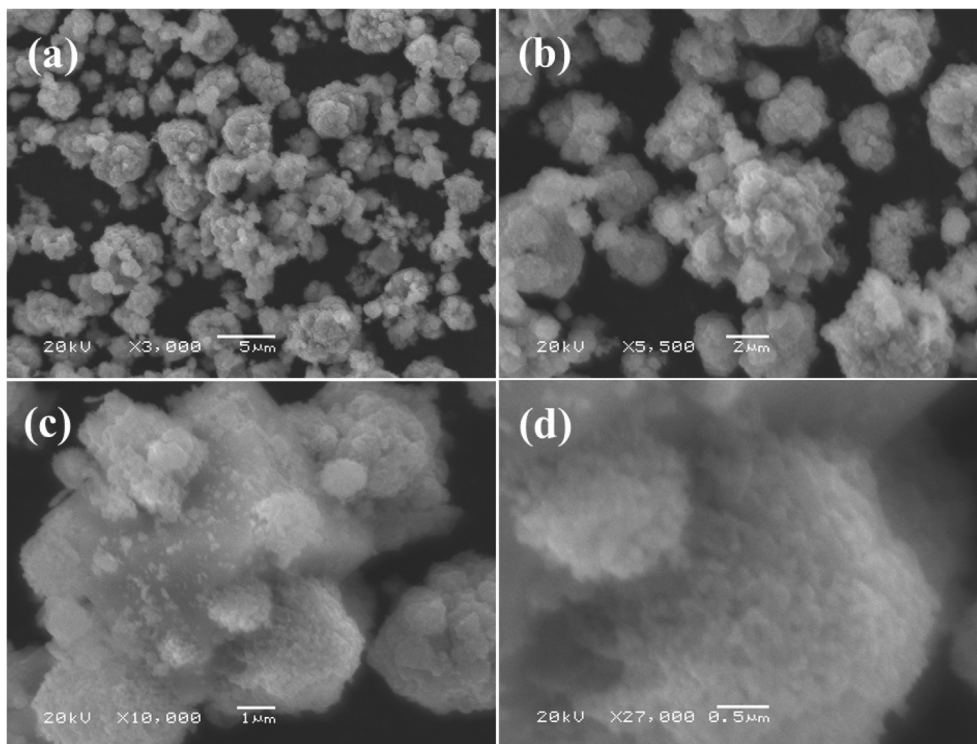


Fig. 1. X-ray diffraction (XRD) pattern of the prepared cobalt oxide nanoparticles ( $\text{Co}_3\text{O}_4\text{NPs}$ ).



**Fig. 2.** Scanning electron microscopy (SEM) images of cobalt oxide nanoparticles ( $\text{Co}_3\text{O}_4\text{NPs}$ ): (a-b) illustrates low magnified images whereas (c-d) shows the high magnified image, which depicts the surface morphology of the cobalt oxide nanoparticles ( $\text{Co}_3\text{O}_4\text{NPs}$ ), the average size of each NP is  $\sim 33 \pm 1$  nm.

NPs surfaces are smooth, clear and consisted with the SEM (Fig. 2) images.

3.2.3. (c) FTIR results

To know the foot prints of utilized chemicals with functional groups, FTIR spectroscopy was utilized in the range of 400–

4000  $\text{cm}^{-1}$ . A wide and shallow peak ranges between 3200 and 3600  $\text{cm}^{-1}$  illustrates the O–H stretching mode whereas an intense peak was observed at 1633  $\text{cm}^{-1}$  for H–O–H molecule (Fig. 4)). The absorption peak at  $\sim 665$   $\text{cm}^{-1}$  is correlated to O–C–O absorption and band at 574  $\text{cm}^{-1}$  depict the Co–O vibration metal oxygen group. From the observed FTIR data it's confirm that no any other band was observed related to other functional group in the spectrum, which shows the purity of the material (Divyapriya et al., 2019, El-Dossoki et al., 2020).

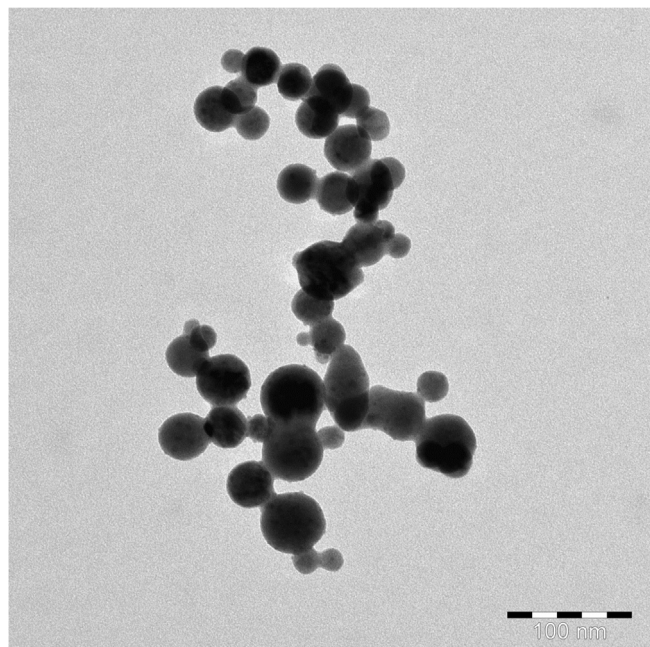


**Fig. 3.** Transmission electron microscopy (TEM) displayed the low magnification image of the cobalt oxide nanoparticles ( $\text{Co}_3\text{O}_4\text{NPs}$ , size  $\sim 33$  nm) synthesized at  $\sim 90$  °C.

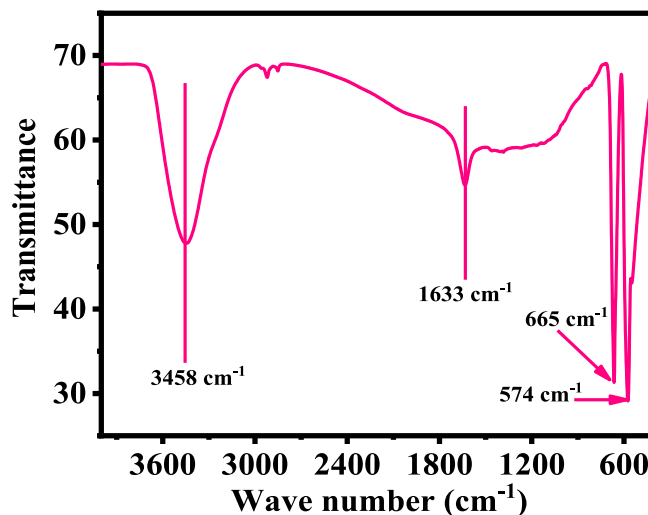


**Fig. 4.** Typical Fourier transform infra-red (FTIR) spectroscopy of grown cobalt oxide nanoparticles ( $\text{Co}_3\text{O}_4\text{NPs}$ ).

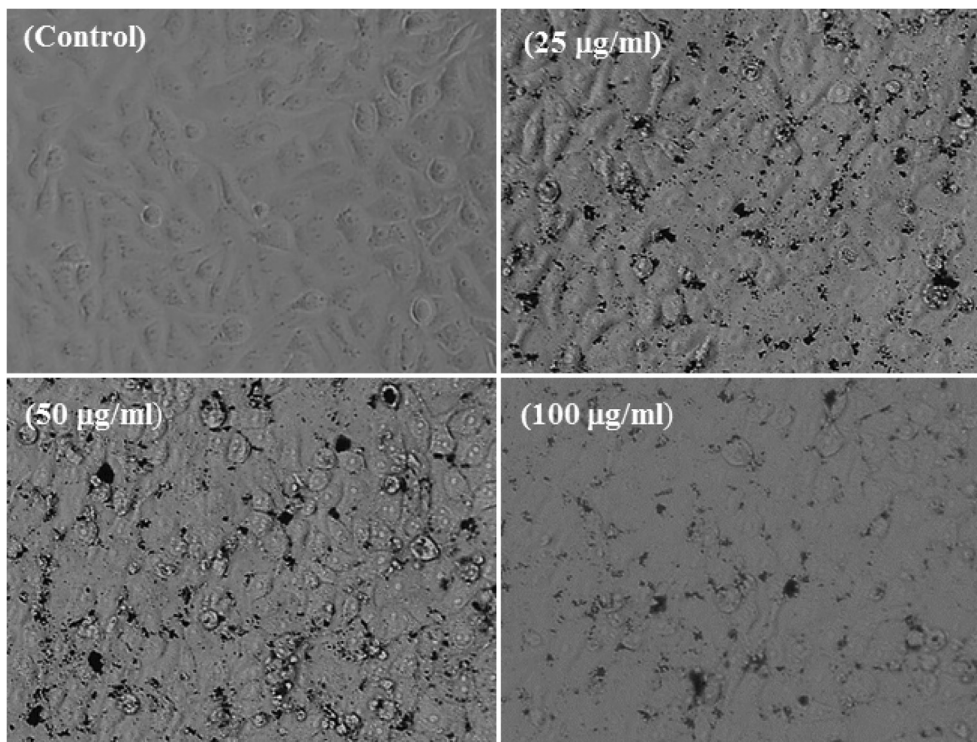


Fig. 5. Structural change in MCF-7 cells with exposed to cobalt oxide nanoparticles (Co<sub>3</sub>O<sub>4</sub>NPs) for 24 h. Images were taken under the phase contrast inverted microscope.

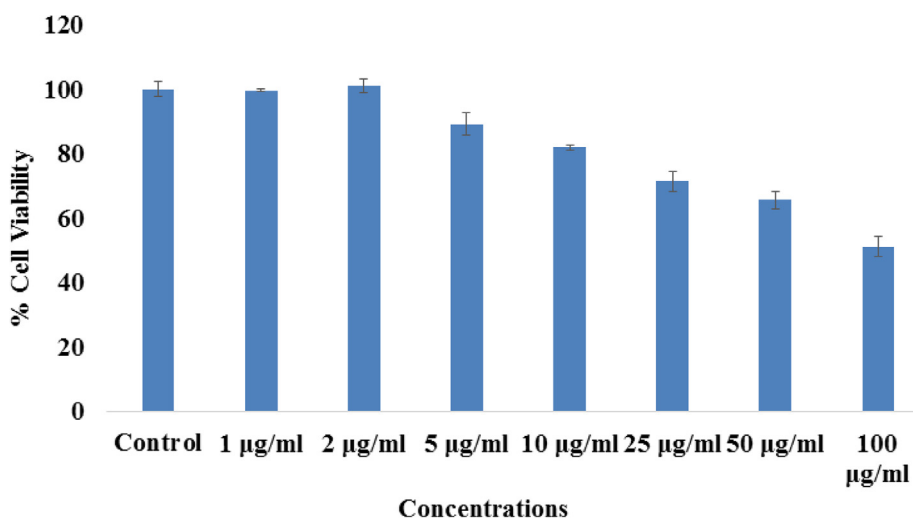


Fig. 6. The study of cytotoxicity via MTT assay in MCF-7 cells succeeding the exposure of cobalt oxide nanoparticles (Co<sub>3</sub>O<sub>4</sub>NPs) for 24 h. The experiments were conducted in triplicate manner (Mean ± SD triplicate).

3.3. Morphological change of cancer cells (MCF-7) with Co<sub>3</sub>O<sub>4</sub>NPs

The cancer cells (MCF-7) were cultured and their morphological evaluation was observed via microscopy at 24 h incubation periods with a number of concentrations (25, 50 and 100 µg/mL) ranges of Co<sub>3</sub>O<sub>4</sub>NPs (Fig. 5). The images were captured for MCF-7 cancer cells and used as control and for their interactions with different concentrations of Co<sub>3</sub>O<sub>4</sub>NPs respectively (Fig. 5). It's evident that initially the cells were nucleated and once their confluences were reached to their optimum level (~70–80%), treated with the Co<sub>3</sub>O<sub>4</sub>NPs with different concentrations (25, 50 and 100 µg/mL) and analyzed. From the obtained images, it reveals that there is not much noteworthy alternation was observed at an initial range of concen-

tration 25 µg/mL, but once this range of concentration of Co<sub>3</sub>O<sub>4</sub>NPs upsurges to 50 to 100 µg/mL, the growth of cells was much influenced with Co<sub>3</sub>O<sub>4</sub>NPs and it was dose dependent. At low concentration 25 µg/mL its doesn't shows any change in cells morphology, whereas at 50 and 100 µg/mL, the cells was destroyed (Fig. 5). From the microscopic images it's very clear that cells were damaged with the Co<sub>3</sub>O<sub>4</sub>NPs.

3.4. The induced cytotoxicity (MTT assay) with processed Co<sub>3</sub>O<sub>4</sub>NPs

As mentioned in the material and methods that the control (MCF-7) and treated (MCF-7 cells with Co<sub>3</sub>O<sub>4</sub>NPs) sample of cells were exposed in a range of different concentrations (ranges

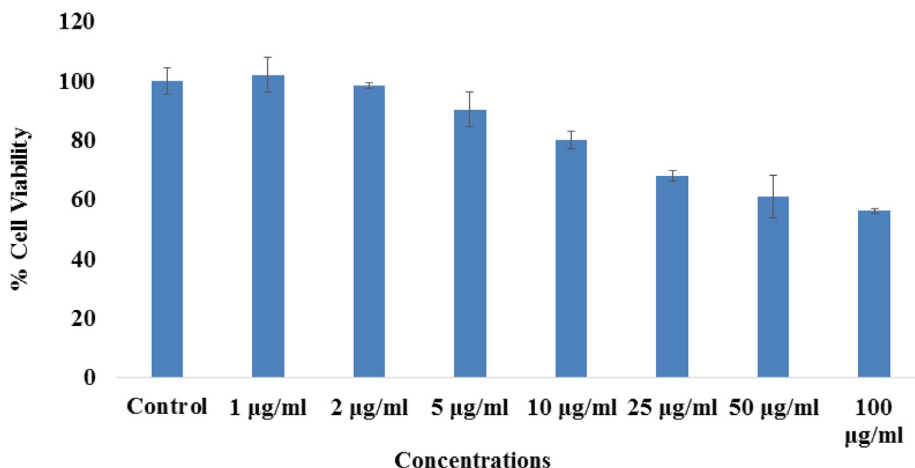


**Fig. 7.** The study of cytotoxicity via NRU assay in MCF-7 cells succeeding the exposure of cobalt oxide nanoparticles ( $\text{Co}_3\text{O}_4\text{NPs}$ ) for 24 h. The experiments were conducted in triplicate manner (Mean  $\pm$  SD triplicate).

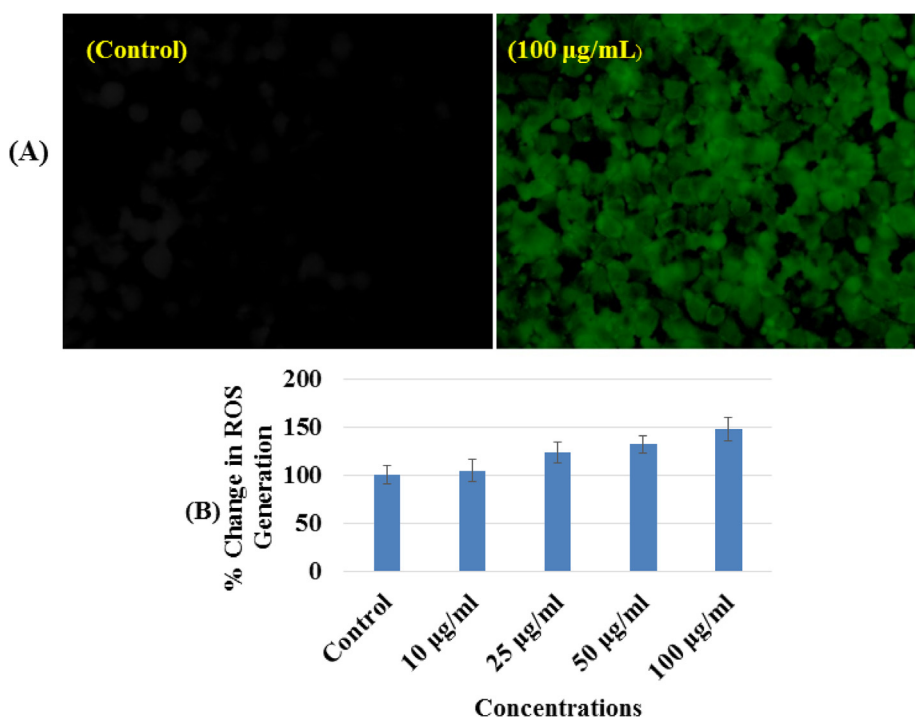


**Fig. 8.** (A) Representative images of cobalt oxide nanoparticles ( $\text{Co}_3\text{O}_4\text{NPs}$ ) induced reactive oxygen species (ROS) generation in MCF-7 cells exposed for 24 h. (B) Percent change in reactive oxygen species (ROS) generation with MCF-7 at different concentrations of cobalt oxide nanoparticles ( $\text{Co}_3\text{O}_4\text{NPs}$ ) for 24 h.

from 1 to 100  $\mu\text{g/ml}$ ) for 24 h incubation. Cells cytotoxicity was examined via MTT assay. From the obtained data it shows that the viability of cancer cells was diminished with  $\text{Co}_3\text{O}_4\text{NPs}$  and data was concentration/dose-dependent. For the MCF-7 cells viability, MTT assay was decreases at 24 h 99%, 101%, 89%, 81%, 71%, 65% and 51% (Fig. 6) for the concentrations of 1, 2, 5, 10, 25, 50 and 100  $\mu\text{g/ml}$  correspondingly ( $p < 0.05$  for each). From the data its shows that at initial concentration, it was not much affected whereas when the concentration of processed material is increase the cytotoxicity was much influenced.

### 3.5. Cytotoxicity study via NRU assay in MCF-7 cells with $\text{Co}_3\text{O}_4\text{NPs}$

Including MTT assay, the cytotoxic measurement was also confirmed with and without  $\text{Co}_3\text{O}_4\text{NPs}$  via NRU assay as detailed in the materials and method. A similar trend was also observed in NRU assay. From the obtained data it depict that the viability of cancer cells at initial doses of  $\text{Co}_3\text{O}_4\text{NPs}$  is not much affected, whereas once the concentration/doses increases, the cancer cells was diminished. For the MCF-7 cells, NRU assay was decreases at 24 h 102%, 98%, 90%, 80%, 67%, 60% and 56% (Fig. 7) for the concentrations of 1, 2, 5, 10, 25, 50 and 100  $\mu\text{g/ml}$  correspondingly ( $p < 0.05$  for each).

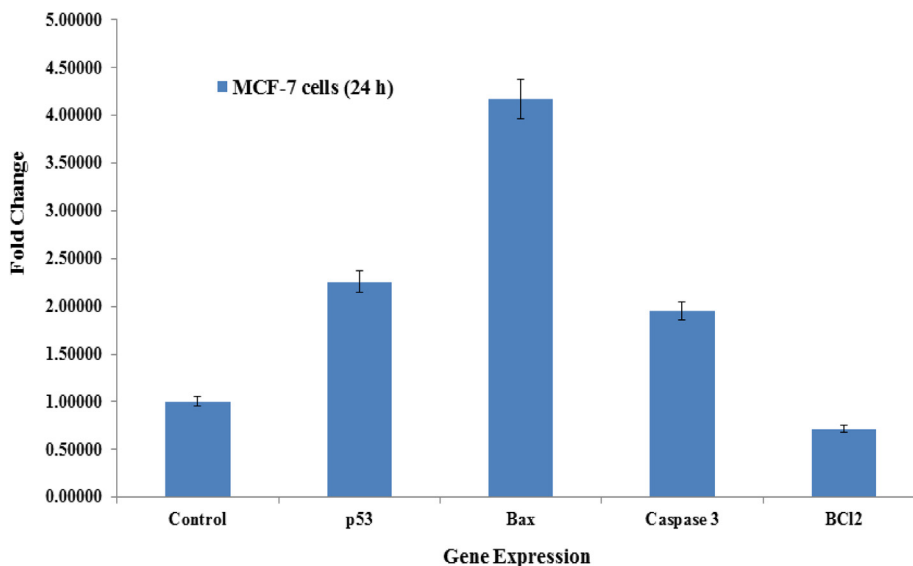


**Fig. 9.** mRNA expression of apoptosis marker genes by real-time polymerase chain reaction (RT-PCR) analysis in MCF-7 cells with cobalt oxide nanoparticles ( $\text{Co}_3\text{O}_4\text{NPs}$ ) at 50 mg/mL concentration for 24 h. RT-PCR data was achieved with Roche Light Cycler<sup>®</sup>480 soft-ware (version 1.5). The glyceraldehyde 3-phosphate dehydrogenase (GAPDH) gene was used as a control to normalize data. The data is accessible as the mean  $\pm$  SD of three identical experiments with three replicates manner. \*Significantly different compared with the control group ( $p < 0.05$  for each).

### 3.6. Induced ROS generation in MCF-7 with $\text{Co}_3\text{O}_4\text{NPs}$

A sequential trend for ROS generation was detected in MCF-7 cells after the exposure of  $\text{Co}_3\text{O}_4\text{NPs}$  at 100  $\mu\text{g}/\text{mL}$  concentrations for 24 h (Fig. 8). The ROS is increases with the  $\text{Co}_3\text{O}_4\text{NPs}$  and it's evident from the images (Fig. 8A) as compared to control cells. An increase of  $148.00 \pm 11.7\%$  was observed in ROS generation at 100  $\mu\text{g}/\text{mL}$ , as compared to control (Fig. 8B).

### 3.7. Gene expressions study

The RT-PCR was utilized to understand the mRNA levels of apoptotic marker genes (e.g. p53, Bax, caspase-3 and  $\text{BCl}_2$ ) in MCF-7 cells interacted with  $\text{Co}_3\text{O}_4\text{NPs}$  oxide at 50  $\mu\text{g}/\text{mL}$  for 24 h. A significant change was observed in mRNA levels in apoptotic markers (p53, Bax, caspase-3 and  $\text{BCl}_2$ ) genes in MCF-7 cells, when exposure with  $\text{Co}_3\text{O}_4\text{NPs}$  (Fig. 9). The mRNA of tumor suppression gene supports the apoptosis induction by foreign material (NPs) and observed the enzymatic activities of caspase-3 at the concentrations of 50  $\mu\text{g}/\text{mL}$ . In all the selected gene, the observations shows that the expression were in up-regulation except  $\text{BCl}_2$  and the fold changes for the p53 (2.2), Bax (4.1), Casp3 (1.9) and  $\text{BCl}_2$  (0.71) respectively (Fig. 9). The Results showed that NPs induced the apoptotic enzymes (caspase-3) in a dose-dependent manner (Fig. 9).

## 4. Conclusions

The summary of the present work shows that the  $\text{Co}_3\text{O}_4\text{NPs}$  (size  $\sim 33 \pm 1$  nm) were prepared via solution process and well characterized. The  $\text{Co}_3\text{O}_4\text{NPs}$  were utilized at very low concentration (1 to 100  $\mu\text{g}/\text{mL}$ ) against MCF-7 cancer cells, which signifies that the cytotoxicity of MCF-7 cells is dose-dependent and influence against cancer cells validated via MTT and NRU assays. The apoptosis or cells death caused with  $\text{Co}_3\text{O}_4\text{NPs}$  enhance at an optimized doses of nanostructure concentration. The current work implies the possibility to use processed nanostructures will be much effective against cancer cells and will be useful as an inorganic based nanodrug. To testify the prepared nanostructures, a

detailed investigation as well as their sustainability under biological environments is required. The study epitomize that  $\text{Co}_3\text{O}_4\text{NPs}$  induces the cytotoxicity, apoptosis in MCF-7 cancer cells via p53, Bax, and caspase pathways. It also expected that  $\text{Co}_3\text{O}_4\text{NPs}$  to be intervened via ROS generation and oxidative stress. The overall recovered data suggest that the NPs are responsible to control the growth of cancer cells. Due to very small size it can be quickly and easily reach to the cells organelles as compared to other complex structures of drugs. The utilization of inorganic based nano structured materials for cancer studies can be possible to reduce the cost of the drugs also these nanostructured based studies reduces the anxiety of surgery for deprived patient.

### Declaration of Competing Interest

The authors declare that they have no known competing financial interests or personal relationships that could have appeared to influence the work reported in this paper.

### Acknowledgement

The authors are grateful to the Deanship of Scientific Research, King Saud University for funding through Vice Deanship of Scientific Research Chairs.

## References

- American Cancer Society. Breast Cancer Facts & Figures 2019-2020. Atlanta: American Cancer Society, Inc. 2019. <https://www.cancer.org/content/dam/cancer-org/research/cancer-facts-and-statistics/breast-cancer-facts-and-figures/breast-cancer-facts-and-figures-2019-2020.pdf>
- Arsalan, N., Kashi, E.H., Hasan, A., Doost, M.E., Rasti, B., Paray, B.A., Nakhjiri, M.Z., Sari, S., Sharifi, M., Shahpas, K., Akhtari, K., Haghghat, S., Falahati, M., 2020. Exploring the Interaction of Cobalt Oxide Nanoparticles with Albumin, Leukemia Cancer Cells and Pathogenic Bacteria by Multispectroscopic, Docking, Cellular and Anti bacterial Approaches. *Inter. J. Nanomed* 15, 4607–4623.
- Askarinejad, A., Bagherzadeh, M., Morsali, A., 2010. Catalytic performance of  $\text{Mn}_2\text{O}_4$  and  $\text{Co}_3\text{O}_4$  nanocrystals prepared by sonochemical method in epoxidation of styrene and cyclooctene. *Appl. Surf. Sci.* 256 (22), 6678–6682.
- Bejarbaneh, M., Moradi-Shoeili, Z., Jalali, A., Salehzadeh, A., 2020. Synthesis of Cobalt Hydroxide Nano-flakes Functionalized with Glutamic Acid and

- Conjugated with Thiosemicarbazide for Anticancer Activities Against Human Breast Cancer Cells. *Biol. Trace Elem. Res.* 198 (1), 98–108.
- Bossi, E., Zanella, D., Gornati, R., Bernardini, G., 2016. Cobalt oxide nanoparticles can enter inside the cells by crossing plasma membranes. *Sci. Rep.* 6, 22254.
- Boing, L., Vieira, M.d.C.S., Moratelli, J., Bergmann, A., Guimarães, A.C.d.A., 2020. Effects of exercise on physical outcomes of breast cancer survivors receiving hormone therapy—A systematic review and meta-analysis. *Maturitas* 141, 71–81.
- Borenfreund, E., Puerner, J.A., 1985. Toxicity determined in vitro by morphological alterations and neutral red absorption. *ToxicologyLett* 24 (2-3), 119–124.
- Bray, F., Jemal, A., Grey, N., Ferlay, J., Forman, D., 2012. Global cancer transitions according to the Human Development Index (2008–2030): a population-based study. *Lancet Oncol.* 13 (8), 790–801.
- Cammarata, F.P., Forte, G.I., Broggi, G., Bravatà, V., Minafra, L., Pisciotta, P., Calvaruso, M., Tringali, R., Tomasello, B., Torrisi, F., Petringa, G., Cirrone, G.A.P., Cuttone, G., Acquaviva, R., Caltabiano, R., Russo, G., 2020. Molecular Investigation on a Triple Negative Breast Cancer Xenograft Model Exposed to Proton Beams. *Int. J. Mol. Sci.* 21 (17), 6337. <https://doi.org/10.3390/ijms21176337>.
- Chen K., Wei J., Ge C., Xia W., Shi Y., Wang H., Jiang X., 2020. Application of autoplanning in radiotherapy for breast cancer after breast conserving surgery. *Scientific Reports* 10:10927
- Chattopadhyay, S., Chakraborty, S.P., Laha, D., Baral, R., Pramanik, P., Roy, S., 2012. Surface-modified cobalt oxide nanoparticles: new opportunities for anti-cancer drug development. *CancerNano* 3 (1-6), 13–23.
- Cullity, B.D., 1978. *Elements of X-ray Diffraction*. Addison-Wesley, Reading, MA.
- Divyapriya, G., Vijayakumar, K.K., Nambi, I., 2019. Development of a novel graphene/Co<sub>3</sub>O<sub>4</sub> composite for hybrid capacitive deionization system. *Desalination* 451, 102–110.
- Dong, J., Song, L., Yin, J.-J., He, W., Wu, Y., Gu, N., Zhang, Y., 2014. Co<sub>3</sub>O<sub>4</sub> Nanoparticles with Multi-Enzyme Activities and Their Application in Immunohistochemical Assay. *ACS Appl. Mater. Interfaces* 6 (3), 1959–1970.
- El-Dossoki F., Rady S and Hosny N., 2020. Synthesis of Co<sub>3</sub>O<sub>4</sub> nanoparticles from amino acids mixed ligands and its adsorption properties. *Alfa. J Basic & App Sci* 1:1-12.
- Farhadi, S., Safabakhsh, J., Zaringhadam, P., 2013. Synthesis, characterization, and investigation of optical and magnetic properties of cobalt oxide (Co<sub>3</sub>O<sub>4</sub>) nano particles. *J. Nanostructure in Chem* 3, 69.
- He, X., Zhang, Q., Feng, Y., Li, Z., Pan, Q., Zhao, Y., Zhu, W., Zhang, N., Zhou, J., Wang, L., Wang, M., Liu, Z., Zhu, H., Shao, Z., Wang, L., 2020. Resection of liver metastases from breast cancer: a multicentre analysis. *Clin. Transl. Oncol.* 22 (4), 512–521.
- Huang, X., Cai, H., Zhou, H., Li, T., Jin, H., Evans, C.E., Cai, J., Pi, J., 2021. Cobalt oxide nanoparticle-synergized protein degradation and phototherapy for enhanced anticancer therapeutics. *Acta Biomaterialia* 121, 605–620.
- Iqbal, S., Fakhar-e-Alam, M., Atif, M., Amin, N., Ali, A., Shafiq, M., Ismail, M., Hanif, A., Farooq, W.A., 2020. Photodynamic therapy, facile synthesis, and effect of sintering temperature on the structure, morphology, optical properties, and anticancer activity of Co<sub>3</sub>O<sub>4</sub> nanocrystalline materials in the HepG2 cell line. *J. Photochem and Photobiology A: Chem* 386, 112130. <https://doi.org/10.1016/j.jphotochem.2019.112130>.
- Jarestan, M., Khalatbari, K., pouraei, A., Sadat Shandiz, S.A., Beigi, S., Hedayati, M., Majlesi, A., Akbari, F., Salehzadeh, A., 2020. Preparation, characterization, and anticancer efficacy of novel cobalt oxide nanoparticles conjugated with thiosemicarbazide. *Biotech* 10 (5). <https://doi.org/10.1007/s13205-020-02230-4>.
- Jose J., Kumar R., Harilal S., Mathew GE., Parambi DGT., Prabhu A., Uddin M.S., Aleya L., Kim H., Mathew B., 2020. Magnetic nanoparticles for hyperthermia in cancer treatment: an emerging tool, *Environmental Sci.Poll.Res* 27:19214-19225.
- Karupiah, C., Palanisamy, S., Chen, S.-M., Veeramani, V., Periakaruppan, P., 2014. A novel enzymatic glucose biosensor and sensitive non-enzymatic hydrogen peroxide sensor based on graphene and cobalt oxide nanoparticles composite modified glassy carbon electrode. *Sens. Actuators, B* 196, 450–456.
- Li, J., Li, M., Tian, L., Qiu, Y., Yu, Q., Wang, X., Guo, R., He, Q., 2020. Facile strategy by hyaluronic acid functional carbon dot-doxorubicin nanoparticles for CD44 targeted drug delivery and enhanced breast cancer therapy. *Inter. J. Pharmaceutics* 578, 119122. <https://doi.org/10.1016/j.ijpharm.2020.119122>.
- Li, W.Y., Xu, L.N., Chen, J., 2005. Co<sub>3</sub>O<sub>4</sub> Nanomaterials in Lithium-Ion Batteries and Gas Sensors. *Adv. Func. Mater* 15 (5), 851–857.
- Mauro, M., Crosera, M., Pelin, M., Florio, C., Bellomo, F., Adami, G., Apostoli, P., Palma, G.D., Bovenzi, M., Campanini, M., Filon, F.L., 2015. Cobalt Oxide Nano particles: Behavior towards Intact and Impaired Human Skin and Keratinocytes Toxicity. *Int. J. Environ. Res. Public Health* 12 (7), 8263–8280.
- Mosmann, T., 1983. Rapid colorimetric assay for cellular growth and survival: application to proliferation and cytotoxicity assays. *J. Immunol. Methods* 65 (1-2), 55–63.
- Nardin, S., Mora, E., Varughese, F.M., Avanzo, F.D., Vachanaram, A.R., Rossi, V., Saggia, C., Rubinelli, S., Gennari, A., 2020. Breast Cancer Survivorship, Quality of Life, and Late Toxicities. *Front Oncol.* 10, 864.
- Packiaraj, R., Devendran, P., Venkatesh, K.S., Asath bahadur, S., Manikandan, A., Nallamuthu, N., 2019. Electrochemical Investigations of Magnetic Co<sub>3</sub>O<sub>4</sub> Nano particles as an Active Electrode for Supercapacitor Applications. *J. Super conductivity and Novel Magnetism* 32 (8), 2427–2436.
- Papis, E., Rossi, F., Raspanti, M., Dalle-Donne, I., Colombo, G., Milzani, A., Bernardini, G., Gornati, R., 2009. Engineered cobalt oxide nanoparticles readily enter cells. *ToxicologyLett* 189 (3), 253–259.
- Rauwel, E., Arag, S.A., Salehi, H., Amorim, C.O., Cuisinier, F., Guha, M., Rosario, M.S., Rauwel, P., 2020. Assessing Cobalt Metal Nanoparticles Uptake by Cancer Cells Using Live Raman Spectroscopy. *Inter. J. Nanomed* 15, 7051–7062.
- Siddiqui, M.A., Saquib, Q., Ahamed, M., Farshori, N.N., Ahmad, J., Wahab, R., Khan, S. T., Alhadlaq, H.A., Musarrat, J., Al-Khedhairi, A.A., Pant, A.B., 2015. Molybdenum nanoparticles-induced cytotoxicity, oxidative stress, G2/M arrest, and DNA damage in mouse skin fibroblast cells (L929). *Colloids Surf. B: Biointerfaces* 125, 73–81.
- Siddiqui, M.A., Singh, G., Kashyap, M.P., Khanna, V.K., Yadav, S., Chandra, D., Pant, A. B., 2008. Influence of cytotoxic doses of 4-hydroxynonenal on selected neuro transmitter receptors in PC-12 cells. *Toxicol In Vitro.* 22 (7), 1681–1688.
- Siddiqui, M.A., Kashyap, M.P., Kumar, V., Al-Khedhairi, A.A., Musarrat, J., Pant, A.B., 2010. Protective potential of trans-resveratrol against 4-hydroxynonenal induced damage in PC12 cells. *Toxicol. In Vitro* 24 (6), 1592–1598.
- Sivachidambaram, M., Vijaya, J.J., Kaviyarasu, K., Kennedy, L.J., Al-Lohedan, H.A., Jothi Ramalingam, R., 2017. novel synthesis protocol for Co<sub>3</sub>O<sub>4</sub> nanocatalysts and their catalytic applications. *RSC Adv* 7 (62), 38861–38870.
- Vennela, A.B., Mangalaraj, D., Muthukumarasamy, N., Agilan, S., Hemalatha, K.V., 2019. Structural and Optical Properties of Co<sub>3</sub>O<sub>4</sub> Nanoparticles Prepared by Sol-gel Technique for Photocatalytic Application. *Int. J. Electrochem. Sci* 14, 3535–3552.
- Wahab, R., Dwivedi, S., Umar, A., Singh, S., Hwang, I.H., Shin, H.-S., Musarrat, J., Al-Khedhairi, A.A., Kim, Y.-S., 2013. ZnO Nanoparticles Induce Oxidative Stress in Cloudman S91 Melanoma Cancer Cells. *J. Biomed Nanotech* 9 (3), 441–449.
- Wahab, R., Siddiqui, M.A., Saquib, Q., Dwivedi, S., Ahmad, J., Musarrat, J., Al-Khedhairi, A.A., Shin, H.-S., 2014. ZnO nanoparticles induced oxidative stress and apoptosis in HepG2 and MCF-7 cancer cells and their antibacterial activity. *Colloids Surf. B: Biointerfaces* 117, 267–276.
- Zhao, J., Riediker, M., 2014. Detecting the oxidative reactivity of nanoparticles: a new protocol for reducing artifacts. *J Nanopart Res.* 16 (7), 2493.